Printing of Patterned, Engineered E. coli Biofilms with a Low-Cost 3D Printer

Schmieden, Dominik T.; Basalo Vázquez, Samantha J.; Sangüesa, Héctor; Van Der Does, Marit; Idema, Timon; Meyer, Anne S.

DOI
10.1021/acssynbio.7b00424

Publication date
2018

Document Version
Accepted author manuscript

Published in
ACS Synthetic Biology

Printing of patterned, engineered *E. coli* biofilms with a low-cost 3D printer

Dominik T. Schmieden[1], Samantha J. Basalo Vázquez[1], Héctor Sangüesa[1], Marit van der Does[1], Timon Idema[1], Anne S. Meyer[1,2,*]

[1] Department of Bionanoscience, Kavli Institute of Nanoscience, Delft University of Technology, 2629 HZ Delft, The Netherlands

[2] Department of Molecular Genetics, Erasmus University Medical Center, 3015 CN Rotterdam, The Netherlands

Abstract

Biofilms can grow on virtually any surface available, with impacts ranging from endangering the lives of patients to degrading unwanted water contaminants. Biofilm research is challenging due to the high degree of biofilm heterogeneity. A method for the production of standardized, reproducible, and patterned biofilm-inspired materials could be a boon for biofilm research and allow for completely new engineering applications. Here, we present such a method, combining 3D printing with genetic engineering. We prototyped a low-cost 3D printer that prints bioink, a suspension of bacteria in a solution of alginate that solidifies on a calcium-containing substrate. We 3D-printed *Escherichia coli* in different shapes and in discrete layers, after which the cells survived in the printing matrix for at least one week. When printed bacteria were induced to form curli fibers, the major proteinaceous extracellular component of *E. coli* biofilms, they remained adherent to the printing substrate and stably spatially patterned even after treatment with a matrix-dissolving agent, indicating that a biofilm-mimicking structure had formed. This work is the first demonstration of patterned, biofilm-inspired living materials that are produced by genetic control over curli formation in combination with spatial control by 3D printing. These materials could be used as living, functional materials in applications such as water filtration, metal ion sequestration, or civil engineering, and potentially as standardizable models for certain curli-containing biofilms.

Keywords

3D printing, synthetic biology, biofilm, curli, bioprinting

Biofilms are aggregates of microbial cells surrounded by a self-produced matrix[1]. The formation of a biofilm allows pathogenic bacteria to resist medical treatment[2] or to colonize surfaces such as catheters or implants [3–5], posing a serious risk to patients. Biofilm research thus frequently focuses on combatting nefarious biofilms[6,7], control of biofilm formation[8], patterning of model biofilms[9,10], and biofilm-induced corrosion[11]. Conversely, biofilms are used for beneficial applications such as wastewater treatment[12], bioleaching[13,14], or as living materials for potential applications like bioremediation[15]. Biofilms are highly heterogeneous, leading to uneven distributions of *e. g.* biomass, nutrients, or metabolic products[12], which in turn leads to physiological heterogeneity of the

constituent cells. Genetically variant sub-populations and persister cells have been identified that allow biofilms to re-grow after treatments that largely destroy the biofilm, for example by the immune system or disinfectants[16]. Even genes closely involved in biofilm formation are not necessarily expressed in all cells of the biofilm. DePas *et al.*[17] observed two populations of cells in rugose (wrinkled) biofilms of uropathogenic *E. coli* UTI89: one population expressing an extracellular matrix of amyloid fibers and cellulose at the biofilm surface, while the second population in the inner regions of the biofilm did not express extracellular matrix components. In order for biofilm-inspired living materials to be useful tools for engineering and research, a tight control over the spatial arrangement of the cells, as well as formation of extracellular matrix components, will be required. In this paper, we demonstrate a method that combines 3D printing with genetic control over biofilm formation as a first step in this direction.

While 3D printers are widely used in tissue engineering to arrange eukaryotic cells in arbitrary shapes[18,19], the first bacterial 3D printers for macroscale structures have only recently been developed. Lehner *et al.*[20] suspended bacteria in a solution of alginate, a polymer that forms a gel upon complexation of calcium ions. When this solution was printed onto calcium-containing agar plates with a 3D printer adapted for bacterial cells, multilayered bacteria gels in various shapes could be produced with sub-millimeter precision. Diffusion of nutrients from the substrate allowed the cells to survive for at least two days, and controllable expression of a gene was achieved with a chemical inducer. Thereafter, Schaffner *et al.*[15] created 3D-printed gels containing *Pseudomonas putida* to generate a living material for the degradation of phenol. *Acetobacter xylinum* was also printed to produce bacterial cellulose on a three-dimensional surface, demonstrating a new strategy of materials production with the potential to be used in personalized medicine. However, while these methods excel at arranging cells in a 3D polymeric matrix, the development of a biofilm by the bacteria is uncontrolled, and the stability of the printed bacteria is limited by the chemistry of the matrix polymers[21].

Here, we solve these problems by printing engineered *E. coli* cells that form biofilms in the presence of an inducer. In nature, the switch from planktonic to biofilm growth occurs when *E. coli* faces stress conditions, such as nutrient or salt limitation, or low temperatures[22]. Amyloid fibers called curli[23] form the major proteinaceous component of the extracellular matrix, which can also include cellulose and other polysaccharides, depending on strain and growth conditions[22]. Curli fibers consist of the secreted protein CsgA, which self-assembles[24] on the membrane nucleator protein CsgB[25] to form fibers that interconnect biofilm cells and adhere to surfaces. Curli gene expression is complex, involving proteins encoded in two operons: *csgBAC* and *csgDEFG*[26]. CsgD acts as a positive regulator of curli formation and other biofilm components, while CsgE, F, and G are involved in the export and folding of CsgA and CsgB[27].

In this paper, we demonstrate a novel method for 3D printing patterned biofilm-inspired materials of engineered *E. coli* cells. When engineered cells were induced to express the CsgA protein after printing, they formed artificial biofilms that protected the cells from being washed away with a gel-dissolving agent. Furthermore, we prototyped a cost-effective 3D printer for bacteria made from K'NEX parts that is capable of printing our engineered bacteria in stable, layered 3D structures. The combination of biofilm-forming bacteria with 3D printing could lead to the development of reproducible, standardized biofilms for research and testing to complement existing *in vitro* methods[28]. 3D printing could also allow for the precise patterning of mixed cultures in a hydrogel

environment, for example, to study interactions between pathogens and eukaryotic cells. Furthermore, when combined with genetic or protein engineering, this technique could be used to print completely new, living materials for bio-engineering applications in biotechnology, medicine, or civil engineering.

Results and discussion

The Biolinker, a cost-effective 3D printer for bacteria

In order for engineered biofilms to serve as living materials for engineering applications, precise control over biofilm spatial patterning is needed, which can be achieved by 3D printing. 3D printers built or refitted for high-resolution cell printing have previously been developed successfully[18,20,29,30]. Here, we aimed at building a 3D printer ("The Biolinker") that could serve both as a scientific instrument and as an educational tool, while being cost-effective and consisting of easily obtainable parts. Modular toy construction systems such as Lego or K'NEX are inexpensive and known to many students from their own childhood, and their component pieces are frequently already available to educators, potentially further lowering the price. We developed the Biolinker using K'NEX parts, since K'NEX offers many combinable pieces for building structures with moving parts, such as beams, connectors, gears, chains, and DC motors.

We assembled K'NEX parts to build a frame containing a printhead located overtop of a 2D-stage, which can hold printing substrates. The K'NEX structure was combined with standard electronic components allowing for the controllable motion of the printing stage (Figure 1a). While commercial 3D printers typically use stepper motors to actuate the stage, we employed K'NEX DC motors for the ease of interfacing the motors with the K'NEX frame. The chains connecting the stage to the motors must be installed under sub-maximal tension to prevent breaking the connections between the K'NEX parts of the stage frame, which leads to a delay of about 1 s between switching on the motor and the start of the stage movement (Supporting Figure 1). This delay can be compensated for by delaying the start of the pump that extrudes the bacteria. The speed and direction of rotation of the stage motors and the pump are controlled in an automated, coordinated manner by two Arduino boards, and commands are sent by an external computer running our self-written control software. For improved spatial precision of bacterial deposition, ultrasound sensors report to the control software on the stage position in both the x- and y-directions.

In order to 3D print with bacteria, we need an extrusion mechanism that is non-lethal to cells. In accordance with our aim of affordability, we constructed a DIY peristaltic pump by using publicly available design specifications. This peristaltic pump moves liquids through the printhead (Figure 1b) with precise control over the extrusion flow rate (Supporting Figure 2). However, without a shape-preserving agent that transforms the extruded liquid into a gel, the printed shapes would quickly lose resolution upon spreading of the liquid on the substrate surface. The Biolinker pump thus extrudes "bioink," which is a mixture of bacteria, liquid growth medium, and alginate. Agar plates serve as printing substrates. Prior to printing, a calcium chloride solution is spread onto the plates. Upon printing of the bioink onto the calcium-impregnated printing surface, the alginate molecules of the bioink complex with the calcium ions, polymerizing the bioink into a solid hydrogel that holds the bacteria in place[20].

The Biolinker allows for the printing of simple bioink shapes in 2D (outlines or filled), *e. g.* rectangles, triangles, or even letters such as “T” or “U” (Figure 1c). Printed 2D shapes can be extended into layered 3D shapes after manually raising the syringe tip of the printhead. Different line widths can be produced by changing the pumping speed, allowing a minimum line width of approximately 2 mm (Figure 1d). While the pump can run arbitrarily slowly, a minimum flow rate of approximately 0.33 mL/min was required to produce continuous printing. The width of a multilayered line increased fractionally with each layer added, by an average of approximately 14% (Figure 1d). This increase in width is likely caused by a decrease in calcium ion concentration with higher distance from the printing substrate, allowing the printed bioink to spread out for a longer period of time before gelation occurs. Along the length of printed lines, the width can vary due to different distances between the syringe tip and the agar surface since it is difficult to produce agar plates with completely level surfaces (see thinner sections in Figure 1c).

The Biolinker combines classical engineering, electronics, and biology in a cost-effective DIY manner, making it an interdisciplinary educational tool. Toy kits such as K’NEX or Lego have already been used successfully at the school- and university-level to enable the hands-on teaching of natural science subjects or architecture[31,32]. Excluding the external computer, the components of the Biolinker cost about €350 (of which €220 for non-K’NEX parts), making it, to our knowledge, the cheapest 3D printer for cells to date. All printer experiments in this work were performed with the Biolinker, but for applications requiring higher precision, the K’NEX components could easily be replaced with a commercial, albeit more expensive, DIY 3D printing kit[20].

Bacteria can survive for extended periods of time in alginate gels

In order to produce printed biofilms, the deposited bacteria have to survive in the alginate gels for extended periods of time to allow for biofilm formation. Furthermore, depending on the application, the generation of bacterial products should be sustainable over a longer duration and controllable with chemical inducers added to the printing substrate. When printing multiple stacked layers of bioink on a calcium-containing substrate, we saw gelation of the ink within seconds for the first layer and up to 5 minutes for the fifth layer, showing that calcium ions can diffuse freely from the substrate to the upper layers. To investigate whether printed bacteria can also be furnished effectively with nutrients and inducers diffusing from the printing substrate, we printed bacteria expressing an inducible blue fluorescent protein onto LB-agar plates. The agar contained the appropriate inducer for production of the fluorescent protein, while the bioink contained none. We monitored the fluorescence of the bacteria-containing gel over a timespan of two weeks using confocal microscopy, revealing robust fluorescence during the first week after the printing (Supporting Figure 3). This result demonstrates that gene expression in printed bacteria can be controlled by inducers present in the substrate.

To gauge the effect of gel encapsulation on bacterial survival, we determined the number of colony forming units (CFU) in printed bioink over a time span of 12 days by dissolving samples with citrate solution and incubating on LB-agar plates (Figure 2). In order to compare the viability in gel cultures to liquid cultures, we also printed bioink onto LB-agar plates that did not contain calcium, so that gelation was not triggered. Prior to CFU determination, these liquid cultures were treated with either citrate or PBS, allowing for observation of the influence of the citrate treatment on viability. The number of colony forming units in gels remained stable within approximately one order of magnitude for 7-8 days after printing before declining sharply. Liquid cultures showed the highest

number of colony forming units one day after the print, after which the number of CFUs declined to approximately the level of the gel samples. The viability of these liquid cultures remained stable at a level comparable to the gel cultures for the following 6 days before dying off. Citrate-treated cultures consistently showed fewer CFUs than non-treated ones, suggesting a mildly toxic effect from the 10-minute citrate treatment.

From the fluorescence and viability experiments, we conclude that, in this setup, printed bacteria are useful for experimentation and applications for roughly one week after printing. The main limiting factors of bacterial survival are likely nutrient depletion, accumulation of waste products, and drying of the gels and plates. Drying can be delayed by sealing the plates with plastic wrap and supplementation of water. If bacteria would have to be kept alive in bioink gels for a longer time, fresh nutrients could be supplied and waste products could be removed by submerging the printed gels in growth medium, supplied with calcium chloride to avoid gel dissolution[21].

Bacteria can be 3D printed in discrete layers

Depending on the application, printed 3D structures should retain their layering, and only minimal mixing of bacteria should occur between the layers. In order to observe the mixing behavior of structures printed with the Biolinker, we printed a layer of bioink containing yellow fluorescing bacteria on top of a layer of bioink containing blue fluorescing bacteria. To facilitate imaging, a glass coverslip served as the printing substrate instead of an agar plate. After each printing cycle, we added calcium chloride solution to solidify the alginate in the bioink. Thirty minutes after solidification of the second layer, we imaged the printed material along the z-axis using fluorescent confocal microscopy (Figure 3a-c). Quantification of the distributions of the different colors of bacterial fluorescence revealed that the bacteria mixed on a stretch of approximately 16 µm along the z-axis (maximum to maximum, Figure 3d). When the bioink layers were not solidified with calcium ions, the two types of bacteria were thoroughly intermixed, and a 3D structure failed to form (Figure 3e). The alginate bioink chemistry is thus an essential prerequisite to produce layered 3D structures. ~~Therefore, the calcium-alginate bioink chemistry allows the Biolinker to print patterned, 3-dimensional structures with z-axis spatial resolution on the order of 10-20 µm.~~

CsgA expression is rate-limiting for curli formation

In order to 3D-print biofilms using the Biolinker, we wished to engineer our printed cells to inducibly overexpress curli fiber proteins. Curli fibers are constructed outside the cell from CsgA monomers[24]. Each fiber is attached to a CsgB outer membrane protein[25]. We applied a mathematical modeling approach to determine whether both CsgA and CsgB would need to be overexpressed in order to promote robust, inducible curli fiber growth. We used a simple kinetic model to estimate the growth rate of the fibers, from which we could estimate the extracellular CsgA production rate *r*. We have:

$$\frac{dM}{dt} = n\,P - \gamma_M M - \mu M,$$

$$\frac{dC}{dt} = k_t M - \gamma_C C - \mu C - k_e C,$$

$$r = k_e C$$

where *M* and *C* are the number of *csgA* mRNA and CsgA protein molecules per cell, *n* the copy number of the (plasmid containing the) *csgA* gene, *P* the promoter activity, γ_M and γ_C the degradation

rate of *csgA* mRNA and CsgA protein, μ the growth rate of the cells, k_t the translation rate, and k_e the CsgA export rate constant, which we assumed to be constant since the CsgA transporter CsgG is ATP-independent[33]. Under steady-state conditions, the time derivatives and the growth rate are equal to zero. We then solved for the extracellular CsgA production rate as a function of the promoter activity and the various constants:

$$r = \frac{k_e}{k_e + \gamma_C} \frac{n\, k_t}{\gamma_M} P \approx \frac{n\, k_t}{\gamma_M} P$$

where we made the approximation that the export rate constant is significantly larger than the degradation rate of CsgA protein. We estimated the CsgA production rate by adding a GFP reporter to a rhamnose-inducible CsgA construct and measuring the steady-state bacterial fluorescence upon rhamnose induction (see Supporting Information). For a rhamnose concentration of 0.2%, we determined an extracellular CsgA production rate of 2 molecules per second for a cell, with $n \approx 200$ copies of the *csgA* plasmid. When we raised the rhamnose concentration to 0.5%, the production rate increased to 3 molecules per second. Since the number of CsgB anchors on the outer membrane is in the range of $10^2 - 10^3$ [34], we concluded that the CsgA production is the rate-limiting step for the curli formation and that placing the *csgA* gene behind an inducible promoter will allow us to control the curli growth rate.

Biofilm formation can be controlled by exogenous expression of CsgA

Our modeling results suggested that control over biofilm formation can be achieved by genetic control of the *csgA* gene alone, while all other proteins involved in biofilm formation can be left untouched. To validate this result experimentally, we transformed a *csgA* knockout strain (*E. coli ΔcsgA*) with either a plasmid for inducible expression of CsgA or a control plasmid without the *csgA* gene. Due to the lack of genomically-encoded CsgA, these strains are not able to form biofilms naturally[35]. We tested these strains for biofilm formation in a microtiter plate assay[36]. Overnight bacteria cultures were diluted 1:100 with LB medium and grown in 96-well microtiter plates for five days at room temperature in the presence of the inducer rhamnose or the non-inducing sugar glucose. Planktonic cells were washed away, and remaining biofilm was stained with Crystal Violet. The Crystal Violet dye was then dissolved in ethanol and detected via optical density at 595 nm. For both strains, we measured a significantly higher amount of biofilm when the bacteria were grown in the presence of the inducer (Mann-Whitney U-test, $p < 0.0005$). Bacteria not expressing CsgA showed a 20% increase in biofilm formation in the presence of the inducer, while bacteria containing the plasmid for CsgA production showed a robust 131% increase in biofilm formation upon induction (Figure 4). These results confirm that our plasmid encoding for inducible control of CsgA expression alone was indeed sufficient to induce the formation of engineered *E. coli* biofilms in solution.

CsgA-expressing bacteria allow the production of patterned biofilms

In order to create useful model biofilms, printed bacteria should form a biofilm-like structure in the alginate matrix that stably links the printed bacteria cells together, even when the alginate is dissolved. The gelation process of alginate is reversible; calcium can be washed out or removed by strong calcium-complexing agents such as citrate, dissolving the gels[37]. To test the efficiency of dissolution of 3D printed alginate gels, we printed samples with different numbers of layers onto agar plates and compared their weight before and after dissolution with sodium citrate (Figure 5). We observed dissolution of 82.1% ± 7.9% (SD) of one-layered gels, 96.5% ± 1.1 % of three-layered

gels, and 96.8% ± 2.1% of five-layered gels, indicating that printed alginate gel can be dissolved nearly completely.

If our printed *E. coli* cells were able to efficiently form curli fibers in an alginate matrix, we would expect that the fibers would stabilize the matrix and take over the role of the alginate, keeping the cells in place upon dissolution of the alginate gel. To test the effect of CsgA expression, *E. coli ΔcsgA* containing either a plasmid for constitutive GFP expression, or a plasmid for constitutive GFP as well as inducible CsgA expression, was added to bioink and printed onto LB-agar plates containing the inducer rhamnose. The bioink was incubated for three days to allow for curli production, and then the total fluorescence of the plates was measured. Subsequently, the alginate gels were treated with sodium citrate solution for an extended period (2 hours) to thoroughly dissolve the alginate matrix, and the total fluorescence of the plates was measured again (Figure 6). Before citrate treatment, both printed gels showed strong fluorescence of similar intensity. After citrate treatment, the total fluorescence of the plate containing printed bacteria lacking CsgA had decreased significantly (paired t-test, $t(9) = -13.2$, $p < 0.0005$), indicating that the bacteria had been largely washed away. In contrast, the fluorescence intensity of plates containing printed CsgA-expressing bacteria was not significantly affected by the citrate treatment ($t(9) = -1.75$, $p = 0.114$). Although this harsh, extended citrate treatment resulted in a significant decrease in bacterial viability (Supporting Figure 6, independent samples t-test, $t(10) = 6.44$, $p = 0.01$), removal of printed alginate gel for engineering applications could be achieved through milder and less cytotoxic strategies such as the use of lower citrate concentrations, alternative chemicals such as EDTA, or submersion of the gel in low-calcium solutions.

To measure the physical stability of printed *E. coli* in a fluorescence-independent manner, we measured the optical density of citrate solutions used for bioink dissolution in order to detect the release of bacteria from printed bioink gels. Following citrate treatment of bioink gels containing CsgA-deficient bacteria, we found that the citrate solution had a mean optical density of 9.2 ± 1.0 (S. D.), which was approximately 50 times higher compared to citrate solutions used to treat bioink gels containing CsgA-expressing cells (Supporting Figure 7, Mann-Whitney U-test, $p = 0.004$). These data indicate that CsgA-deficient cells were released into suspension in large numbers due to the citrate treatment, while CsgA-expressing cells were stably and homogeneously anchored within the bioink gel. These results show that curli fibers can take over the function of alginate as fixation agents for printed bacteria, while at the same time mimicking the extracellular matrix of certain natural *E. coli* biofilms.

We next tested whether CsgA expression would allow our printed bacteria to retain a specific spatially patterned shape. We printed parallel stripes of bioink containing *E. coli* expressing CsgA, as well as stripes of bioink containing *E. coli* not expressing CsgA. After incubation for three days to allow the production of curli fibers, we attempted to dissolve the stripes with a sodium citrate solution. Stripes of bioink containing CsgA-producing *E. coli* maintained their striped pattern (Figure 7a, b, upper panels; Supporting Figure 8), while stripes of CsgA-deficient cells dissolved gradually from the bioink gel surface towards the printing surface until they were largely obliterated (Figure 7c, d, upper panels; Supporting Figure 8). When imaging printed bioink gels using confocal microscopy, we found the bacteria of both genotypes arranged in clusters of varying sizes, ranging from approximately 5-35 μm in length along the longest axis (Figure 7a, c, lower panels). Following citrate treatment, bioink containing CsgA-expressing bacteria appeared more homogeneous than before

treatment, with fewer apparent bacteria clusters (Figure 7b, lower panel). Citrate-treated bioink containing CsgA-deficient cells had retained only a small number of cells directly in contact with the agar surface (Figure 7d, lower panel). The formation of bacteria clusters seen in untreated bioink might have been caused by microcolony growth under spatial constriction by the alginate gel or the developing curli network, with larger clusters potentially arising from the merging of smaller, neighboring clusters. The more homogeneous distribution of cells in citrate-treated bioink containing CsgA-expressing cells may have been due to a loss of integrity of the printed gel following alginate removal, so that the pressure of a microscope cover slip might have introduced imaging artifacts by disturbing the microstructure of the film. In conclusion, these results show that printed engineered biofilms of *E. coli* can remain stably spatially patterned on a macroscopic level even when treated with a strong gel-dissolving agent.

Conclusion

We have developed a new method for 3D printing of stable, patterned bacterial biofilm-inspired materials. While our engineered biofilms do not reproduce every feature of natural biofilms, our method allows for precise control over certain biofilm characteristics, such as spatial arrangement, species composition, and bacterial density. 3D printing could be used to produce standardized, reproducible biofilms for the evaluation of protective anti-biofilm coatings on medical devices, or for the testing of treatments against curli-forming pathogens. Further research is required to establish which features of biofilms of curli-forming bacteria are reproduced by our artificial biofilms, and how printed biofilms compare to other biofilm model systems such as the Calgary biofilm device and others[28,38]. Schaffner *et al.* have demonstrated that oxygen limitation impacts the metabolic activity of bacteria in 3D-printed gels[15]. To deal with limitations in nutrient and oxygen supply, 3D printing could be used to arrange bacteria in combination with water channels, such as those found in natural biofilms[39]. We would like to note that while we did not observe the emergence of bacteria sub-populations in printed bioink, our results do not necessarily preclude physiological heterogeneity of the cells.

An important feature of 3D printing not available in other biofilm fabrication methods is the possibility to print and arrange different types of bacteria in a controlled fashion in 3D space. Synthetic microbial consortia are increasingly used to investigate bacterial interactions or to create complex synthesis pathways spanning several distinct types of bacteria[40–42]. The controlled spatial arrangement of these interacting bacteria groups could lead to further optimization in interaction-dependent processes[43], for which 3D printing has already been shown to be a promising tool[44]. In foundational research, biofilms can be modeled as layered structures to account for biofilm heterogeneity[45]. 3D printing of biofilms in layers according to model parameters could be a way to validate these models. Finally, curli fibers functionalized with peptide tags[35,46] have recently emerged as new tools for the production of new nanomaterials[47], with diverse potential applications such as electronics[35,48] or bioremediation[49]. 3D printing could make a valuable contribution to these approaches by providing a means of patterning and scale-up of materials production to the micro- and macroscale.

Methods

Chemicals were purchased from VWR Netherlands or Sigma Netherlands unless otherwise indicated.

Bacterial strains, plasmids, and culture

Escherichia coli MG1655 *PRO ΔcsgA ompR234*[35,50], henceforth called *E. coli ΔcsgA*, served as the experimental strain for experiments with inducible CsgA expression.

Liquid cultures of *E. coli* Top 10 and *E. coli ΔcsgA* cells were grown at 37 °C under continuous shaking in LB medium unless otherwise indicated. When carrying plasmids, appropriate antibiotics were added to the growth medium (25 µg/mL ampicillin, 25 µg/mL kanamycin, 34 µg/mL chloramphenicol). For chemical induction of genes, inducer concentrations were 1 mM IPTG, 50 ng/mL anhydrotetracycline, and 0.2% (w/v) or 0.5% (w/v) rhamnose or 0.5% (w/v) glucose (for non-inducing conditions).

Plasmid AM420 is a p15A-derived plasmid carrying an ampicillin resistance gene, a constitutively expressed *lacI* gene, and the gene for the blue fluorescent protein Cerulean (gene sequence originally from pZS2-123[51], Addgene plasmid # 26598) behind an IPTG-inducible lac UV5 promoter[52].

Plasmid AM421 is a pSC101-derived plasmid carrying a kanamycin resistance gene, a constitutively expressed *tetR* gene, and the gene for the yellow fluorescent protein mVenus (gene sequence originally from mVenus N1[53], Addgene plasmid # 27793) behind an anhydrotetracycline-inducible promoter[54].

Plasmid pSB1C3 is the standard iGEM shipping backbone, which contains a ColE1 origin and a chloramphenicol resistance gene. The copy number per cell is between 100 and 300 copies (http://parts.igem.org/Part:pSB1C3).

Plasmid BBa_K1583112 was assembled from pSB1C3 and a rhamnose-inducible promoter from BBa_K914003 which controls the *csgA* gene from BBa_K1583000 and the GFPmut3b[55] gene from BBa_E0040.

Plasmid AM401 was constructed by inserting the biobrick BBa_I20270 (encoding for GFP behind a constitutive promoter) into plasmid pSB1C3.

Plasmid AM404 was assembled by inserting the BBa_I20270-part of AM401 into BBa_K1583100 (plasmid pSB1C3 containing a rhamnose-inducible promoter followed by the *csgA* gene).

Sequences of plasmids constructed in this work are accessible online (Supporting Table 1). iGEM plasmid sequences (plasmids pSB1C3 and BBa_ plasmids) can be found in the iGEM Registry of Standard Biological Parts (http://parts.igem.org).

The Biolinker

The frame and stage of the Biolinker were built from various K'NEX and electronic parts (Supporting Tables 2, 3), including two 5 V DC K'NEX motors to move the stage along the x- and y-axes (Supporting Table 4, Supporting Figure 1). These K'NEX motors must run at full speed in order to produce enough torque to prevent unexpected stalling of the stage. The motors are controlled by an Arduino Mega 2560 equipped with an Adafruit Motor Shield (V1). The Biolinker is controlled by sending commands in the form of G-codes (Supporting Table 5) via a USB serial interface from a computer. A graphical user interface (GUI) was programmed in Processing. Source codes for the Arduino drivers and the GUI have been deposited on Github (https://github.com/dominikschmieden/biolinker).

The senders and receivers of ultrasound sensors (HC SR-04) were detached, connected to their original circuit boards by cables, and attached facing each other to the stage and the frame. This modification allows direct transmission of the ultrasound signal from sender to receiver without reflection on a surface. This setup was used to determine the position of the stage in x- and y-direction.

The printhead consists of a syringe tip (Sterican, 19G x 1.5") glued to a K'NEX holder in a central position above the stage's area of movement. The tip was blunted by shortening with pliers and filing down to the un-deformed region of the tube. Bioink is pumped through silicon tubing (VWR DENE 3100103/25, 1 mm inner diameter) by an open-source peristaltic pump (http://www.thingiverse.com/thing:529863). The pump rotor and stator were 3D-printed with a Form 1+ 3D printer (Formlabs). The pump stepper motor is controlled by a separate Arduino Uno board and a DRV8824 motor control chip. Commands from the Arduino Mega board to the pump board are sent via the SCA/SCL ports.

Bioink preparation

Bioink was prepared by growing bacteria overnight in 50 mL LB medium with appropriate antibiotics and inducers, then centrifugation for 5 min at 3600 x g. The cell pellet was re-suspended in 10 mL LB medium and 10 mL sodium alginate (3% w/v). Sodium alginate solutions were heated to their boiling point three times after production and stored at 4 °C to prevent the growth of contaminants. For experiments without bacteria, alginate solutions were dyed with 5 mg/mL of Methylene Blue prior to printing to allow imaging and measurements.

Printing substrates

The printing of bacteria was performed on LB-agar plates (1% w/v), supplemented with appropriate antibiotics and inducers. Liquid agar was poured into plates standing on level surfaces to promote a level agar surface after cooling. Plates were dried overnight at room temperature with the lid half-open. To allow alginate gel solidification, a solution of 0.1 M $CaCl_2$ was spread on the plates prior to printing (1 mL for diameter=135 mm plates, 444 µL for diameter=90 mm plates). $CaCl_2$ was added to solid rather than to liquid agar since addition immediately before printing resulted both in better alginate gelation during the printing process, as well as better dissolution of the alginate gel in calcium removal experiments. For experiments without bacteria, printing substrates were prepared by dissolving 1% agar in water. After pouring, solidification, and drying, the $CaCl_2$ solution was spread on the plates as described above.

Characterization of line widths

The width of alginate gel lines printed with the Biolinker was determined by printing dyed alginate onto agar plates (1% in H_2O) along the printer's y-axis at different speed settings. Between prints of different layers, the plates were incubated at 4 °C for 10 min to allow for gel solidification while limiting dye diffusion into the agar. After printing, the plates were imaged, and the layer width was measured at fixed-distance intervals along the lines.

Confocal microscopy

Bioink gels were imaged with a Nikon $A1^+$ fluorescence confocal microscope (For analyzing spatial separation in the z-direction: magnification 200x, 1.95 µm Z direction step size, excitation wavelengths 457/514 nm, detected wavelengths 482/540 nm for Cerulean and mVenus, respectively.

For imaging of bacteria spatial distribution within printed bioink stripes: magnification 1000x, oil immersion, excitation wavelength 488 nm, detected wavelength 540 nm for GFP). Quantification of fluorescence along the Z-axis was performed image by image with the software ImageJ[56].

Print and microscopy of layered bioink structures

Bioink was prepared containing Top10 strains carrying plasmids AM420 (inducible Cerulean) or AM421 (inducible mVenus, 5 mL overnight culture with inducers, 500 µL LB medium, 2 mL 2% (w/v) alginate). Bioink containing AM420 was printed with the Biolinker (extrusion speed 1.6 mL/min) onto an oxygen plasma-treated glass coverslip (30% power for 25 s, Plasma Preen I) and solidified by application of 5 M $CaCl_2$ solution with a pipette on the edges of the alginate gel, allowing for slow diffusion into the gel from the sides without disturbing the gel structure. Before deposition of the second layer of bioink, unbound $CaCl_2$ was removed by flushing the slide with at least 100 mL of tap water. A second layer of bioink containing AM421 was then generated on top of the first layer, using the same technique. The coverslip carrying the gel was placed on a microscope slide, and the gel was sealed with nail polish. Solidification steps with $CaCl_2$ were omitted in the non-gel control. Imaging by confocal microscopy was performed 30 min after solidification of the second layer.

Biofilm formation upon expression of CsgA in microtiter plates

Biofilm formation was measured with a microtiter plate assay[36]. *E. coli ΔcsgA* carrying plasmids AM401 (constitutive GFP) or AM404 (constitutive GFP and rhamnose-inducible CsgA) were grown overnight at 37 °C with shaking at 250 rpm in LB medium supplemented with 34 µg/mL chloramphenicol. Cultures were then diluted 1:100 into 200 µL LB low salt medium (10 g/L tryptone, 5 g/L yeast extract, supplemented with 0.5% (w/v) rhamnose or glucose and 34 µg/mL chloramphenicol) per well of 96-well transparent, flat bottom microtiter plates (Greiner Bio-One 655185). Plates were incubated at 30 °C for five days in a sealed container (with a layer of water below the plates to prevent drying out) to allow biofilm formation. Planktonic cells were removed by washing the plates three times via submerging in tap water and shaking off of the water. Biofilms were stained with 210 µL/well Crystal Violet solution (0.1% w/v in water) for 15 min at room temperature. The dye was removed and the wells washed another three times with water. Residual water was removed by tapping the inverted plate vigorously onto paper towels and air drying. The wells were then filled with 200 µL/well 99% ethanol, covered, and incubated at room temperature for 15 min with shaking at 30 rpm. 100 µL of the ethanol solution was transferred from each well to a new microtiter plate, and O. $D._{590}$ was measured with a Tecan Infinite M200 Pro plate reader. The data were analyzed with Mann-Whitney U tests (see Supporting Information).

Alginate gel dissolution

Calcium ion-permissible dialysis membranes (Spectra/Por 2 Dialysis Tubing, 12-14 kD MWCO, Spectrum Europe B.V., The Netherlands) were placed onto agar plates (1% in H_2O), and the Biolinker was used to print a layer of 2% alginate onto the membrane. After solidification of the alginate, additional layers of alginate were printed on top. For 5-layer samples, 1 mL of $CaCl_2$ solution was layered onto the gels after 3 layers.

To determine gel mass before and after dissolution, the membrane with the alginate gel was lifted off the agar plate, dried briefly with paper tissues, weighed, and replaced onto the dish. The gels were then submerged in 30 mL 0.1 M sodium citrate (adjusted to pH = 7 with NaOH) and incubated

at room temperature on a rotary shaker at 30 rpm for 30 min. After incubation with sodium citrate, the membrane was lifted off again, dried, and weighed as before.

Bacterial survival in printed bioink

Bioink was prepared containing *E. coli ΔcsgA* transformed with plasmid AM401 (constitutive GFP). 2 mL of this bioink was printed onto LB-agar plates (30 mL LB agar per plate, supplemented with chloramphenicol and $CaCl_2$). The plates were sealed with plastic wrap to reduce evaporation and incubated for twelve days at 37 °C. 1 mL of deionized water was added daily to all samples and spread evenly over both the agar and the bioink gel to compensate for the evaporative loss of liquid. No change of water level over the duration of the experiment was observed, so no dilution was assumed. Samples of the gel were taken with a scalpel at different time points. Due to the greater stability of the agar substrate compared to the bioink gel, the bioink could be removed without agar contamination. The extracted gels were weighed, and gel mass was correlated with pumped volume via a pre-determined calibration curve. The gel samples were transferred into 0.5 M sodium citrate solution (pH 7 with NaOH) and adjusted to a concentration of 50 µL pumped bioink per 1 mL gel-citrate mixture. The gels were dissolved by incubation for 10 min at room temperature with occasional vortexing and serially diluted with phosphate-buffered saline (PBS) in 1:10 increments. Samples from these dilutions were plated onto LB plates and incubated overnight at 37 °C. Colonies were counted to determine colony forming units per microliter of pumped bioink.

To investigate the influence of gelation and 10-minute citrate treatment on bacterial survival, 2 mL of bioink was printed as described above, but onto substrate plates containing no $CaCl_2$, leading to a liquid culture on top of the agar surface. These plates were incubated and supplied with water in the same way as the gel samples. Samples were removed by shaking the plates for 1 h at 100 rpm on a rotatory shaker following water addition to re-suspend any sedimented bacteria, and 50 µL of the solution was transferred into 950 µL PBS or into 950 µL 0.5 M sodium citrate solution. After incubation for 10 min, serial dilutions of the samples were prepared and plated as described for the gel samples.

To determine the effect of a two-hour citrate treatment on bacterial survival, 2 mL of bioink containing *E. coli* AM401 (constitutive GFP) was printed onto LB-agar plates containing $CaCl_2$ (resulting in a bioink gel) or not (resulting in a liquid culture on the agar surface). After 3 days of incubation at 37 °C, 20 mL of 0.5 M sodium citrate solution (pH 7 with NaOH) was added to the bioink gel, and 20 mL of PBS was added to the liquid culture. The plates were incubated for 2 hours on a rotatory shaker at 60 rpm to dissolve the bioink gel. 50 µL of the solution was transferred into 950 µL PBS. After incubation for 10 min, serial dilutions of the samples were prepared and plated as described above.

Biofilm formation in alginate gels

Bioink was prepared containing *E. coli ΔcsgA* transformed with AM404 (constitutive GFP, rhamnose-inducible CsgA) or *E. coli ΔcsgA* with plasmid AM401 (constitutive GFP). For the bacteria-free control, only LB medium, alginate, and rhamnose were mixed.

This bioink was printed in a filled, single-layer polygon shape (extrusion speed 2.3 mL/min) onto LB-agar plates (supplemented with $CaCl_2$, 0.5% rhamnose, and chloramphenicol). The plates were incubated for three days at room temperature in darkness. Plate fluorescence was measured with a

GE Typhoon Trio fluorescence scanner (excitation wavelength 488 nm, PMT 450 V, emission filter 520 BP 40, high sensitivity) and averaged over the printed area. The alginate gel was dissolved by the addition of 20 mL 0.5 M sodium citrate (adjusted to pH = 7 with NaOH) for 2 hours with 30 rpm shaking at room temperature in darkness. The liquid was discarded, and plate fluorescence was measured again as before. The significance of differences was analyzed with paired t-tests (see Supporting Information).

Release of bacteria into citrate solution

Bioink was prepared containing *E. coli ΔcsgA* transformed with AM404 (constitutive GFP, rhamnose-inducible CsgA) or *E. coli ΔcsgA* with plasmid AM401 (constitutive GFP). For a bacteria-free control, only LB medium, alginate, and rhamnose were mixed.

Identical parallel lines of these bioinks were printed onto LB-agar plates (supplemented with $CaCl_2$, 0.5% rhamnose, and chloramphenicol). The plates were incubated for 8 days at room temperature, after which the gels were submerged in 10 mL 0.5 M sodium citrate solution (adjusted to pH = 7 with NaOH) for 2 hours with 30 rpm shaking at room temperature. Samples of the liquid were taken, and the optical density at 600 nm determined with an Ultrospec 10 Cell Density Meter (Biochrom, US). 20x dilutions of CsgA(-) samples were measured to reach measurements of O. $D._{600} < 0.5$. The mean O. $D._{600}$ of cell-free bioink (0.02) was subtracted from the O. $D._{600}$ values of the other bioinks.

Supporting Information

The Supporting Information contains a list of g-codes, printer components, printer building instructions, electrical schematics, measured stage characteristics, further modeling explanations, statistical tests, and plasmid information.

Author information

Corresponding Author

*Email: anne@annemeyerlab.org

ORCID

Dominik T. Schmieden: 0000-0002-7766-0053
Samantha J. Basalo Vázquez: 0000-0003-2764-4570
Héctor Sangüesa: 0000-0001-5621-7020
Marit van der Does: 0000-0002-2476-158X
Timon Idema: 0000-0002-8901-5342
Anne S. Meyer: 0000-0002-4164-0122

Author Contributions

D.T.S. designed and performed all experiments except for the measurement of CsgA expression; performed the data analysis; designed, built, programmed, and characterized the Biolinker; and wrote the manuscript except for the modeling sections. S.J.B.V. and M.v.d.D. conceived of the initial idea and design of a K'NEX 3D bioprinter. S.J.B.V. performed and wrote the modeling sections throughout. H.S. and M.v.d.D. measured and analyzed the CsgA expression. T.I. and A.S.M.

supervised the project and assisted in the writing of the paper. All authors read and corrected the manuscript.

Notes

The authors declare no competing financial interests.

Acknowledgments

Escherichia coli MG1655 PRO ΔcsgA ompR2341 was gifted to us by Timothy K. Lu (Department of Biological Engineering, Massachusetts Institute of Technology). Plasmids AM420 and AM421 were constructed and gifted to us by Ferhat Büke. We thank Roland Kieffer, Simon Lindhoud, Victor Marin and Benjamin Lehner for helpful discussions about the printer design, as well as Ilja Westerlaken for assistance in the lab. We acknowledge Jeremie Capoulade for assistance with the confocal microscopy, as well as Jakob Söhl and Ewa Spiesz for help with statistical analyses. For the project idea and initial experiments, we thank the TU Delft 2015 iGEM team: Max van't Hof, Stefan Marsden, Tudor Vlas, Michelle Post, Liana Uilecan, Anne Rodenburg, Esengül Yildirim, Jorine Eeftens, and Helena Shomar Monges. This work was supported by the Netherlands Organization for Scientific Research (NWO/OCW), as part of the Frontiers of Nanoscience program.

Figures

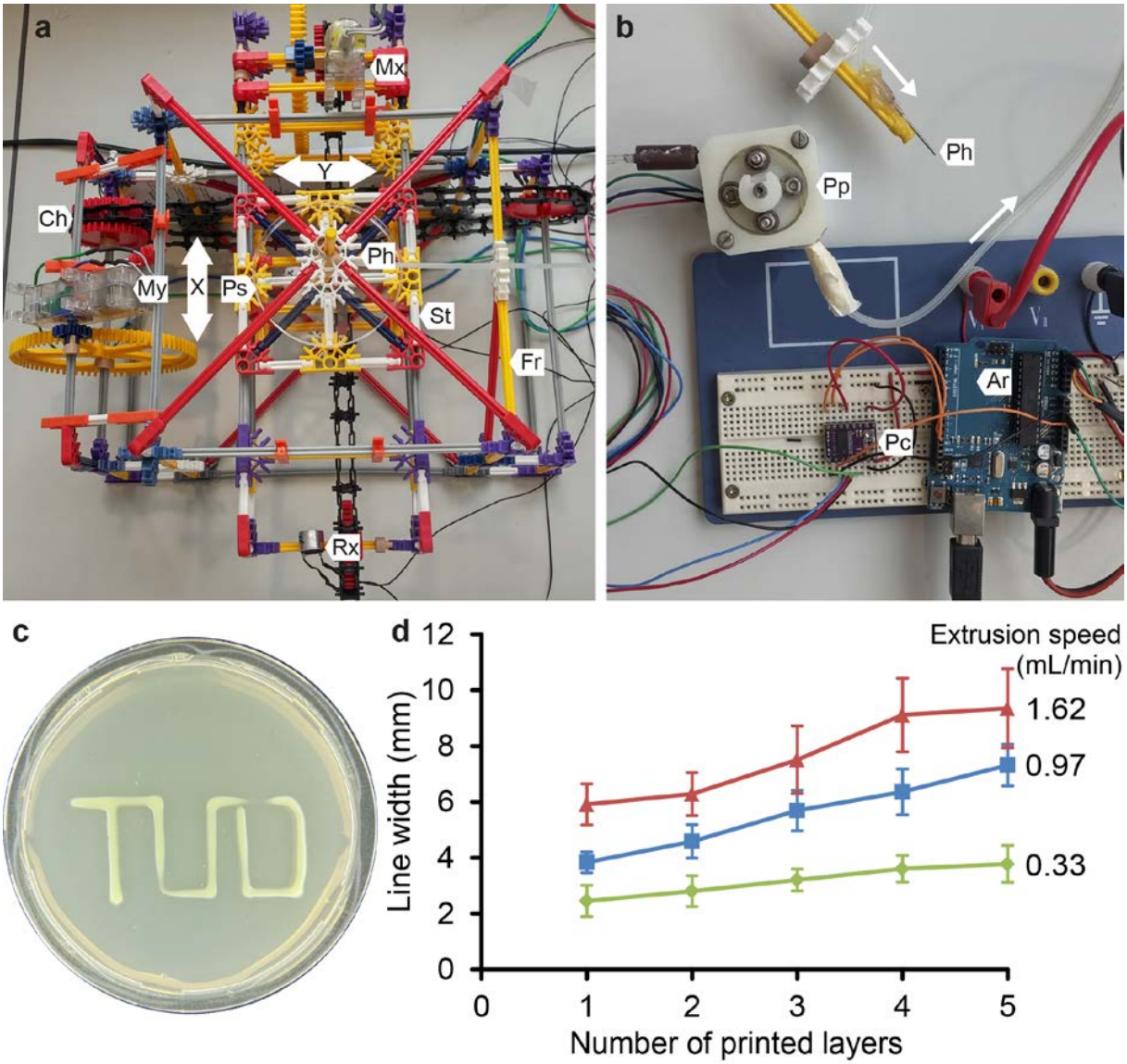

Figure 1. The Biolinker: a 3D printer for bacteria built with K'NEX and electronic parts. (a) Printing stage with frame seen from above, **Mx:** motor x-axis, **My:** motor y-axis, **Ch:** chain, **Ps:** printing substrate, **Ph:** printhead, **St:** printing stage, **Fr:** frame, **Rx:** receiver of x-axis ultrasound sensor. Double-headed arrows indicate axis orientation. **(b)** Printer pump and print head, **Pp:** peristaltic pump, **Ph:** printhead (detached), **Pc:** pump controller, **Ar:** Arduino board. Arrows indicate flow direction. **(c)** Bioink containing green-fluorescing bacteria printed with the Biolinker onto an LB-agar plate. **(d)** Lines containing up to five layers of alginate gel were printed onto agar plates with three different extrusion speeds. Error bars represent the standard deviation.

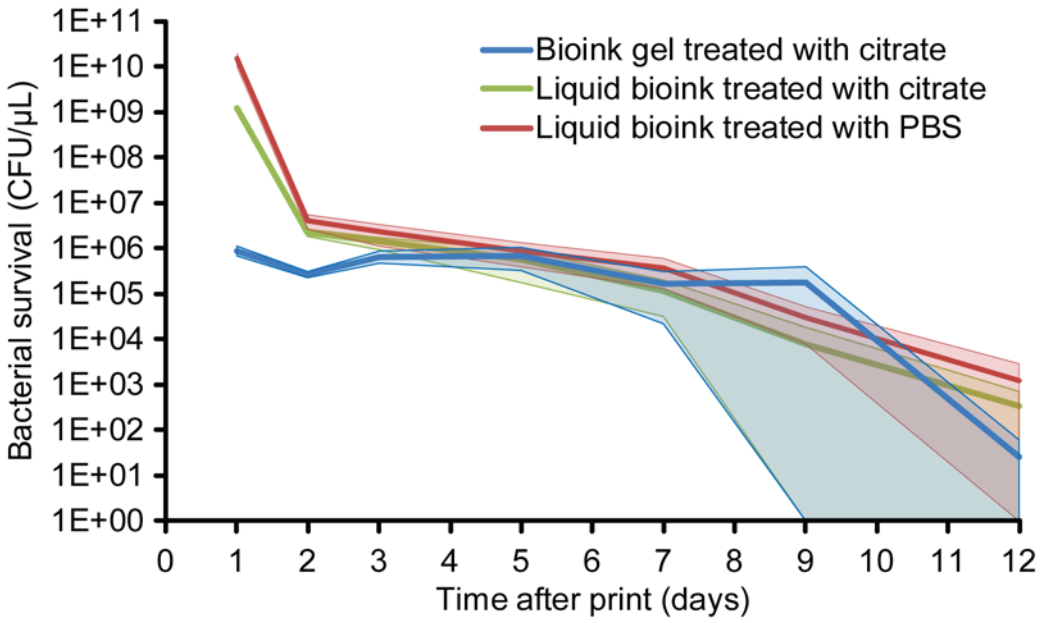

Figure 2. Bacteria in bioink gels remain viable for 7-9 days. Bioink containing *E. coli* AM401 (constitutive GFP) was printed onto LB-agar plates either supplemented with $CaCl_2$, to create solidified bioink gel (blue line), or without $CaCl_2$, to keep the bioink in liquid form on the agar surface (red and green lines). Bioink samples were incubated at 37 °C for 12 days, during which samples were taken and colony forming units determined. Prior to CFU determination, gel samples were dissolved by treatment with sodium citrate solution, and liquid samples were either treated with citrate (green line) or PBS (red line). Shaded areas represent the standard deviations, shown with a lower boundary of 1. n = 3.

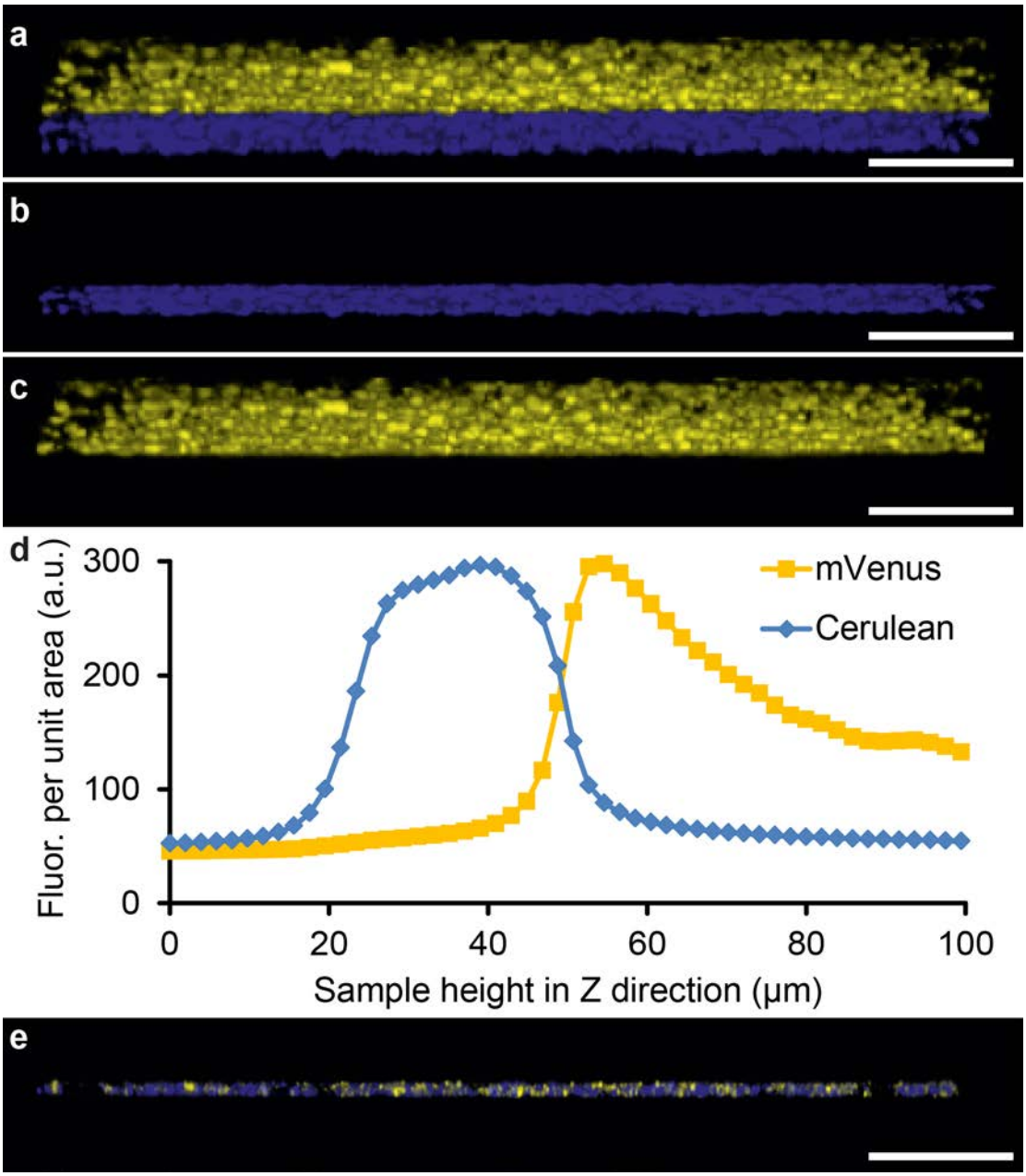

Figure 3. The Biolinker can print bacterial layers with spatial separation in the z-direction. A layer of bioink containing blue fluorescing bacteria was printed on a glass coverslip, followed by a layer of bioink containing yellow fluorescing bacteria. The interface between the layers was examined by confocal microscopy. **(a-d)** The bioink was solidified with Ca^{2+} after each printed layer. **(a)** Composite image of blue and yellow detection channels. **(b)** Blue channel only. **(c)** Yellow channel only. **(d)** Fluorescence per area of (a) measured along the z-axis for each channel separately. **(e)** Bioink layers were printed and imaged as in (a) but without the addition of Ca^{2+} ions (composite image). Scale bars are 100 µm.

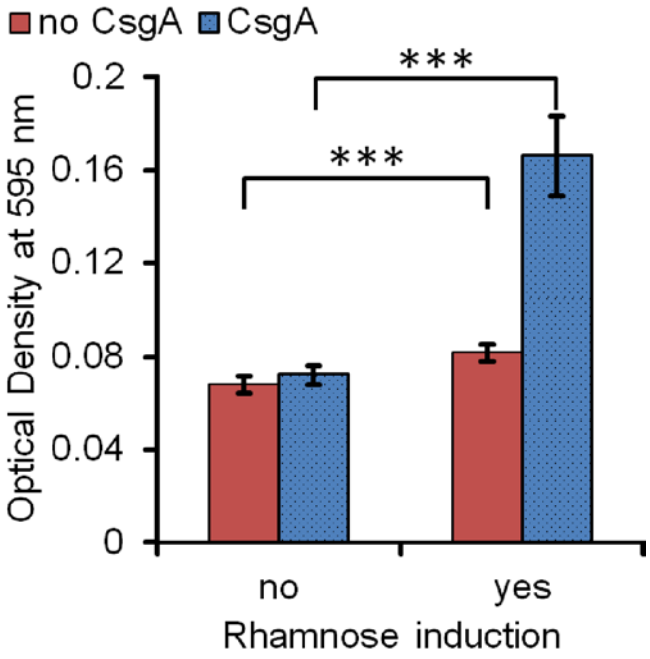

Figure 4. *E. coli ΔcsgA* forms biofilms in solution when induced to express CsgA. *E. coli* ΔcsgA expressing GFP (red) or GFP and rhamnose-inducible CsgA (blue) was grown for five days in the presence or absence of the inducer rhamnose and stained with Crystal Violet. Crystal Violet staining was detected by measuring absorption at O. $D._{595}$ with a spectrophotometer. *** = significant difference ($p < 0.0005$), error bars represent the standard deviation, n = 64.

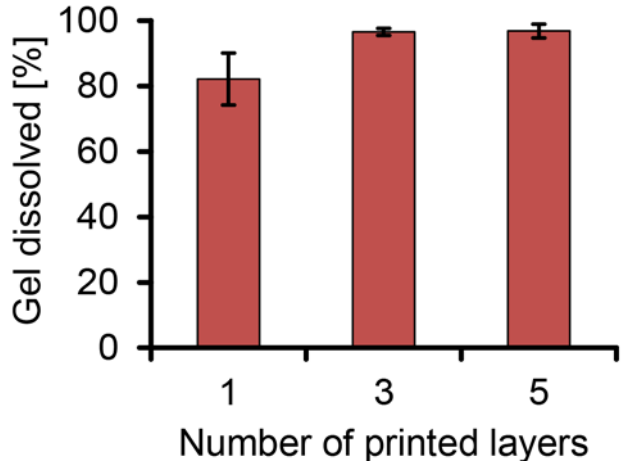

Figure 5. Sodium citrate can dissolve multi-layer printed alginate gels. Alginate (2% w/v) solutions were printed in varying numbers of layers with the Biolinker onto agar plates and allowed to form gels. The alginate was then submerged in 0.5 M sodium citrate. Dissolution efficiency was determined by weighing. Error bars represent the standard deviation, n = 3.

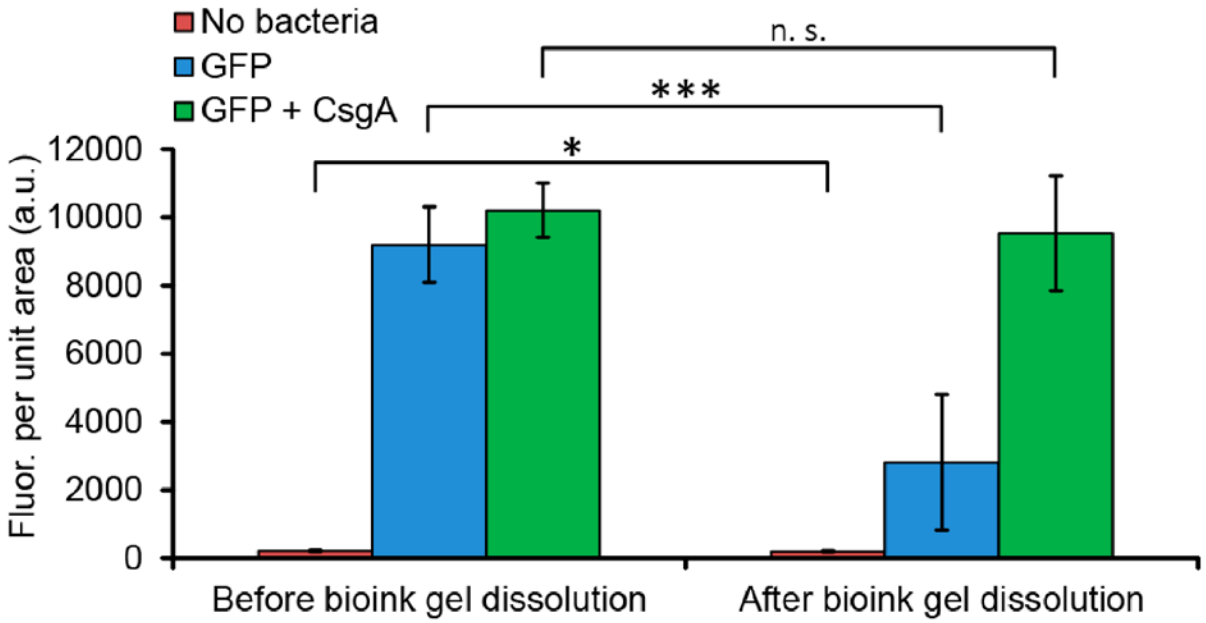

Figure 6. Printed bacteria that express CsgA are protected from alginate gel dissolution. Bioink was printed onto LB-agar plates and allowed to solidify. We printed bioink containing no bacteria (red bars), *E. coli* expressing only GFP (blue bars), or *E. coli* expressing both GFP and CsgA (green bars). The bioink gels were dissolved, and the average plate fluorescence both before and after dissolution was measured with a fluorescence scanner. * = significant difference ($p = 0.014$), *** = significant difference ($p < 0.0005$), n. s. = non-significant difference, error bars represent the standard deviation, $n = 10$.

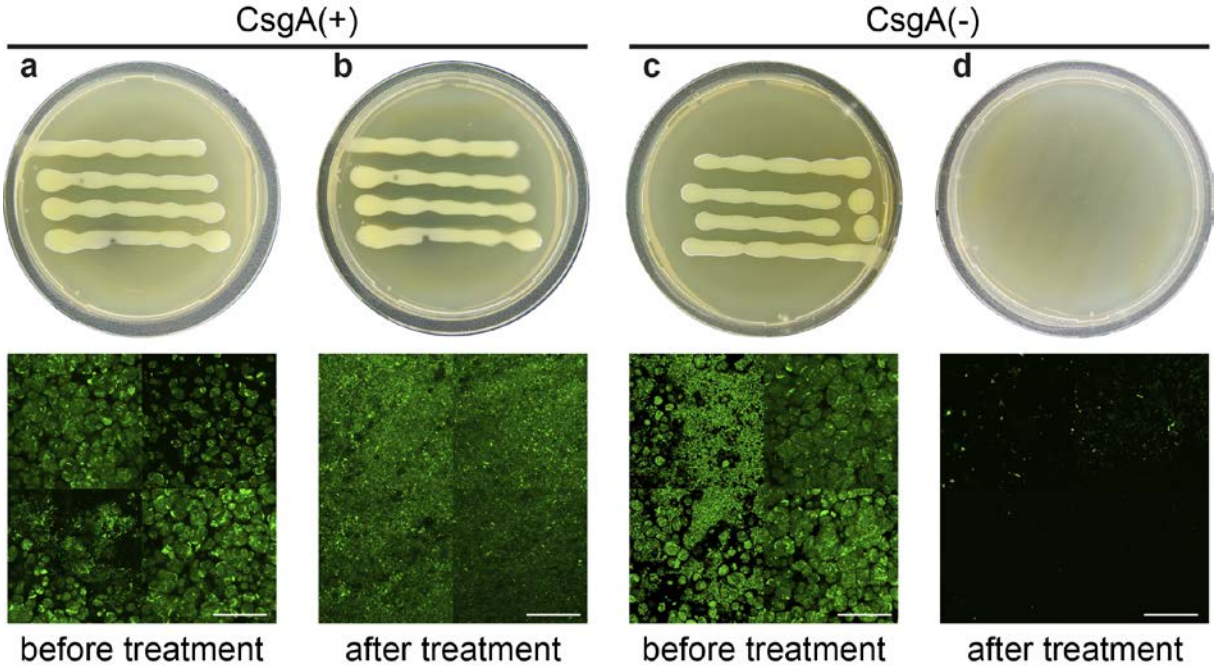

Figure 7. 3D-printed *E. coli* that express CsgA form patterned biofilms that are resistant to the gel-dissolving agent citrate. Bioink containing *E. coli ΔcsgA* either expressing GFP and CsgA **(a, b)** or only GFP **(c, d)** was printed in parallel lines by the Biolinker onto LB-agar plates and allowed to solidify. After incubation for three days at room temperature, the plates were treated with 0.5 M citrate for 2 h to dissolve the alginate gel. **(upper row)** Macroscopic images depicting the entire petri dish. **(lower row)** Representative confocal images, scale bars are 50 µm.

References

(1) Hall-Stoodley, L., Stoodley, P., Kathju, S., Høiby, N., Moser, C., William Costerton, J., Moter, A., and Bjarnsholt, T. (2012) Towards diagnostic guidelines for biofilm-associated infections. *FEMS Immunol. Med. Microbiol.*, *65*, 127–145.

(2) Percival, S. L., Suleman, L., Vuotto, C., and Donelli, G. (2015) Healthcare-associated infections, medical devices and biofilms: risk, tolerance and control. *J. Med. Microbiol.*, *64*, 323–334.

(3) Donlan, R. M. Biofilms on Central Venous Catheters: Is Eradication Possible? In *Bacterial Biofilms*; Romeo, T., Ed.; Springer: Berlin, Heidelberg, 2008, 133–161.

(4) Bauer, T. T., Torres, A., Ferrer, R., Heyer, C. M., Schultze-Werninghaus, C., and Rasche, K. (2002) Biofilm formation in endotracheal tubes. Association between pneumonia and the persistence of pathogens. *Monaldi Arch. Chest. Dis.*, *57*, 84–87.

(5) Francolini, I., and Donelli, G. (2010) Prevention and control of biofilm-based medical-device-related infections. *FEMS Immunol. Med. Microbiol.*, *59*, 227–238.

(6) Li, X.-H., and Lee, J.-H. (2017) Antibiofilm agents: A new perspective for antimicrobial strategy. *J. Microbiol.*, *55*, 753–766.

(7) Sharma, G., Sharma, S., Sharma, P., Chandola, D., Dang, S., Gupta, S., and Gabrani, R. (2016) Escherichia coli biofilm: development and therapeutic strategies. *J. Appl. Microbiol.*, *121*, 309–319.

(8) Nagar, E., and Schwarz, R. (2015) To be or not to be planktonic? Self-inhibition of biofilm development. *Environ. Microbiol.*, *17*, 1477–1486.

(9) Pu, L., Yang, S., Xia, A., and Jin, F. (2017) Optogenetics manipulation enables to prevent biofilm formation of engineered Pseudomonas aeruginosa on surfaces. *ACS Synth. Biol.*, 200–208.

(10) Chen, F., and Wegner, S. V. (2017) Blue Light Switchable Bacterial Adhesion as a Key Step toward the Design of Biofilms. *ACS Synth. Biol.*, 2170–2174.

(11) Li, K., Whitfield, M., and Van Vliet, Krystyn J (2013) Beating the bugs: roles of microbial biofilms in corrosion. *Corros. Rev.*, *31*, 73–84.

(12) Lewandowski, Z., and Boltz, J. P. 4.15 - Biofilms in Water and Wastewater Treatment A2 - Wilderer, Peter. In *Treatise on Water Science*; T1 - 4.15 - Biofilms in Water and Wastewater Treatment A2 - Wilderer, Peter, Ed.; Elsevier: Oxford, 2011, 529–570.

(13) Vera, M., Schippers, A., and Sand, W. (2013) Progress in bioleaching: fundamentals and mechanisms of bacterial metal sulfide oxidation—part A. *Appl. Microbiol. Biotechnol.*, *97*, 7529–7541.

(14) Olivera-Nappa, A., Picioreanu, C., and Asenjo, J. A. (2010) Non-homogeneous biofilm modeling applied to bioleaching processes. *Biotechnol. Bioeng.*, *106*, 660–676.

(15) Schaffner, M., Rühs, P. A., Coulter, F., Kilcher, S., and Studart, A. R. (2017) 3D printing of bacteria into functional complex materials. *Sci. Adv.*, *3*.

(16) Stewart, P. S., and Franklin, M. J. (2008) Physiological heterogeneity in biofilms. *Nat. Rev. Micro.*, *6*, 199–210.

(17) DePas, W. H., Hufnagel, D. A., Lee, J. S., Blanco, L. P., Bernstein, H. C., Fisher, S. T., James, G. A., Stewart, P. S., and Chapman, M. R. (2013) Iron induces bimodal population development by Escherichia coli. *Proc. Natl. Acad. Sci. USA*, *110*, 2629–2634.

(18) Murphy, S. V., and Atala, A. (2014) 3D bioprinting of tissues and organs. *Nat. Biotech.*, *32*, 773–785.

(19) Armstrong, James P. K., Burke, M., Carter, B. M., Davis, S. A., and Perriman, A. W. (2016) 3D Bioprinting Using a Templated Porous Bioink. *Adv. Healthcare Mater.*, *5*, 1724–1730.

(20) Lehner, B. A. E., Schmieden, D. T., and Meyer, A. S. (2017) A straightforward approach for 3D bacterial printing. *ACS Synth. Biol.*, 1124–1130.
(21) Kuo, C. K., and Ma, P. X. (2008) Maintaining dimensions and mechanical properties of ionically crosslinked alginate hydrogel scaffolds in vitro. *J. Biomed. Mater. Res.*, *84A*, 899–907.
(22) Barnhart, M. M., and Chapman, M. R. (2006) Curli Biogenesis and Function. *Annu. Rev. Microbiol.*, *60*, 131–147.
(23) McCrate, O. A., Zhou, X., Reichhardt, C., and Cegelski, L. (2013) Sum of the Parts: Composition and Architecture of the Bacterial Extracellular Matrix. *J. Mol. Biol.*, *425*, 4286–4294.
(24) Wang, X., Smith, D. R., Jones, J. W., and Chapman, M. R. (2007) In Vitro Polymerization of a Functional Escherichia coli Amyloid Protein. *J. Biol. Chem.*, *282*, 3713–3719.
(25) Hammar, M., Bian, Z., and Normark, S. (1996) Nucleator-dependent intercellular assembly of adhesive curli organelles in Escherichia coli. *Proc. Natl. Acad. Sci. USA*, *93*, 6562–6566.
(26) Hammar, M., Arnqvist, A., Bian, Z., Olsén, A., and Normark, S. (1995) Expression of two csg operons is required for production of fibronectin- and Congo red-binding curli polymers in Escherichia coli K-12. *Mol. Microbiol.*, *18*, 661–670.
(27) Evans, M. L., and Chapman, M. R. (2014) Curli biogenesis: Order out of disorder. *Biochim. Biophys. Acta, Mol. Cell Res.*, *1843*, 1551–1558.
(28) Coenye, T., and Nelis, H. J. (2010) In vitro and in vivo model systems to study microbial biofilm formation. *J. Microbiol. Methods*, *83*, 89–105.
(29) Singh, D., Singh, D., and Han, S. S. (2016) 3D Printing of Scaffold for Cells Delivery: Advances in Skin Tissue Engineering. *Polymers*, *8*, 19.
(30) Markstedt, K., Mantas, A., Tournier, I., Martínez Ávila, H., Hägg, D., and Gatenholm, P. (2015) 3D Bioprinting Human Chondrocytes with Nanocellulose–Alginate Bioink for Cartilage Tissue Engineering Applications. *Biomacromolecules*, *16*, 1489–1496.
(31) Gerber, L. C., Calasanz-Kaiser, A., Hyman, L., Voitiuk, K., Patil, U., and Riedel-Kruse, I. H. (2017) Liquid-handling Lego robots and experiments for STEM education and research. *PLoS Biol.*, *15*, e2001413.
(32) Estes, A. C., and Baltimore, C. (2014) Using K'nex to Teach Large Scale Structures to Architects and Construction Students. *121st ASEE Annual Conference & Exposition Proceedings: Indianapolis, IN*.
(33) van Gerven, N., Goyal, P., Vandenbussche, G., Kerpel, M. de, Jonckheere, W., Greve, H. de, and Remaut, H. (2014) Secretion and functional display of fusion proteins through the curli biogenesis pathway. *Mol. Microbiol.*, *91*, 1022–1035.
(34) Wang, X., Zhou, Y., Ren, J.-J., Hammer, N. D., and Chapman, M. R. (2010) Gatekeeper residues in the major curlin subunit modulate bacterial amyloid fiber biogenesis. *Proc. Natl. Acad. Sci. USA*, *107*, 163–168.
(35) Chen, A. Y., Deng, Z., Billings, A. N., Seker, Urartu O. S., Lu, M. Y., Citorik, R. J., Zakeri, B., and Lu, T. K. (2014) Synthesis and patterning of tunable multiscale materials with engineered cells. *Nat. Mater.*, *13*, 515–523.
(36) Zhou, Y., Smith, D. R., Hufnagel, D. A., and Chapman, M. R. (2013) Experimental Manipulation of the Microbial Functional Amyloid Called Curli. *Methods Mol. Biol. (N. Y.)*, *966*, 53–75.
(37) Byrom, D. *Biomaterials: novel materials from biological sources*; Springer, 1991.
(38) Ceri, H., Olson, M. E., Stremick, C., Read, R. R., Morck, D., and Buret, A. (1999) The Calgary Biofilm Device: New Technology for Rapid Determination of Antibiotic Susceptibilities of Bacterial Biofilms. *J. Clin. Microbiol.*, *37*, 1771–1776.

(39) Bjarnsholt, T., Alhede, M., Alhede, M., Eickhardt-Sørensen, S. R., Moser, C., Kühl, M., Jensen, P. Ø., and Høiby, N. (2013) The in vivo biofilm. *Trends Microbiol.*, *21*, 466–474.
(40) Song, H., Ding, M.-Z., Jia, X.-Q., Ma, Q., and Yuan, Y.-J. (2014) Synthetic microbial consortia: from systematic analysis to construction and applications. *Chem. Soc. Rev.*, *43*, 6954–6981.
(41) Zhou, K., Qiao, K., Edgar, S., and Stephanopoulos, G. (2015) Distributing a metabolic pathway among a microbial consortium enhances production of natural products. *Nat. Biotech.*, *33*, 377–383.
(42) Hays, S. G., Patrick, W. G., Ziesack, M., Oxman, N., and Silver, P. A. (2015) Better together: engineering and application of microbial symbioses. *Curr. Opin. Biotechnol.*, *36*, 40–49.
(43) Jagmann, N., and Philipp, B. (2014) Design of synthetic microbial communities for biotechnological production processes. *J. Biotechnol.*, *192*, 293–301.
(44) Connell, J. L., Ritschdorff, E. T., Whiteley, M., and Shear, J. B. (2013) 3D printing of microscopic bacterial communities. *Proc. Natl. Acad. Sci. USA*, *110*, 18380–18385.
(45) Lewandowski, Z., and Beyenal, H. (2003) Biofilm monitoring: a perfect solution in search of a problem. *Water. Sci. Technol.*, *47*, 9.
(46) Nguyen, P. Q., Botyanszki, Z., Tay, Pei Kun R., and Joshi, N. S. (2014) Programmable biofilm-based materials from engineered curli nanofibres. *Nat. Commun.*, *5*, 4945.
(47) Nguyen, P. Q. (2017) Synthetic biology engineering of biofilms as nanomaterials factories. *Biochem. Soc. Trans.*, *45*, 585.
(48) Lovley, D. R. (2017) e-Biologics: Fabrication of Sustainable Electronics with “Green” Biological Materials. *mBio*, *8*, e00695-17.
(49) Tay, Pei Kun R., Nguyen, P. Q., and Joshi, N. S. (2017) A Synthetic Circuit for Mercury Bioremediation Using Self-Assembling Functional Amyloids. *ACS Synth. Biol.*, *6*, 1841–1850.
(50) Prigent-Combaret, C., Brombacher, E., Vidal, O., Ambert, A., Lejeune, P., Landini, P., and Dorel, C. (2001) Complex Regulatory Network Controls Initial Adhesion and Biofilm Formation in Escherichia coli via Regulation of the csgD Gene. *J. Bacteriol.*, *183*, 7213–7223.
(51) Cox, R. S., Dunlop, M. J., and Elowitz, M. B. (2010) A synthetic three-color scaffold for monitoring genetic regulation and noise. *J. Biol. Eng.*, *4*, 10.
(52) Stefano, J. E., Ackerson, J. W., and Gralla, J. D. (1980) Alterations in two conserved regions of promoter sequence lead to altered rates of polymerase binding and levels of gene expression. *Nucleic Acids Res.*, *8*, 2709–2724.
(53) Koushik, S. V., Chen, H., Thaler, C., Puhl III, Henry L., and Vogel, S. S. (2006) Cerulean, Venus, and VenusY67C FRET Reference Standards. *Biophys. J.*, *91*, L99-L101.
(54) Skerra, A. (1994) Use of the tetracycline promoter for the tightly regulated production of a murine antibody fragment in Escherichia coli. *Gene*, *151*, 131–135.
(55) Cormack, B. P., Valdivia, R. H., and Falkow, S. (1996) FACS-optimized mutants of the green fluorescent protein (GFP). *Gene*, *173*, 33–38.
(56) Schneider, C. A., Rasband, W. S., and Eliceiri, K. W. (2012) NIH Image to ImageJ: 25 years of image analysis. *Nat. Meth.*, *9*, 671–675.

Table of contents graphic